A Simple Approach to Estimate Flow-Induced Noise from Steady State CFD Data

Paul Croaker (1), Alex Skvortsov (2) and Nicole Kessissoglou (1)

(1) School of Mechanical & Manufacturing Engineering, The University of New South Wales, Sydney, NSW 2052, Australia
(2) Human Protection and Performance Division, Defence Science and Technology Organisation, Melbourne, Australia

ABSTRACT

A computationally efficient method to approximate the total sound power and far-field acoustic intensity spectra generated by turbulent flow past a rigid body is proposed. The method is based on Proudman's analytical formula for the sound generated by isotropic turbulence. This formula expresses the sound intensity of locally isotropic turbulence for low Mach numbers in terms of the kinetic energy of the turbulence, k, and its dissipation rate, ε. In this work, the approach is extended to non-uniform turbulent flows and the associated acoustic spectra are expressed in terms of the standard steady-state variables, k and ε, conventionally used in computational fluid dynamics (CFD). Since these steady-state variables of turbulent flow are much easier to calculate than the non-stationary turbulent fluctuations used in traditional formulations for the flow sound, this approach dramatically reduces the computational burden of the flow noise calculation. Such a computationally efficient method for predicting flow noise is essential for conducting extensive 'what-if' studies such as shape optimisation to reduce flow noise. The final expressions for the proposed method are calibrated against experimental and numerical data for flow noise of turbulent jets and boundary layers. The method is then applied to study the coefficient of drag and Mach number dependence of the sound generated by flow past a slender body.

INTRODUCTION

Lighthill (1952,1954) derived an acoustic analogy demonstrating that the sound generated by turbulent fluid flow is equivalent to the sound generated by a distribution of quadrupoles computed from the instantaneous velocity fluctuations. Lighthill's acoustic analogy requires transient flow field data from which the acoustic sources are extracted. Prediction of flow induced noise based on Lighthill's acoustic analogy typically uses high fidelity transient CFD simulations such as large eddy simulation (LES), to generate the unsteady turbulent fluctuations required by the method. Wang et al. (2009) and Svennberg and Fureby (2010) have achieved accurate predictions of flow induced noise using such high fidelity approaches. However these high fidelity flow noise prediction methods are computationally expensive with analyses requiring weeks, even months, to complete. This computational expense makes such methods of little use for 'what-if' scenarios such as optimisation studies to reduce flow induced noise.

Building on the work of Lighthill (1952), Proudman (1952) derived analytical expressions to approximate the sound intensity of isotropic turbulence for low Mach numbers in terms of the kinetic energy of the turbulence and its dissipation rate. Based on Proudman's analogy, the flow induced acoustic intensity can be expressed in terms of standard steady-state variables corresponding to the turbulent kinetic energy, k, and dissipation rate, ε, which are conventionally used in CFD. The advantage of this approach is that the flow induced noise can be approximated from steady-state CFD data and hence methods based on Proudman's analogy are much more computationlly efficient than those based on Lighthill's analogy. The computational efficiency of flow noise predictions obtained using Proudman's analogy makes the method extremely attractive for comparative design studies.

This paper presents a $k-\varepsilon$ sound model to approximate the noise generated by turbulent flow past a slender body. The method is based on the work of Proudman (1952) and extended to include the sound produced by a turbulent boundary layer (TBL) acting on a body immersed in turbulent flow. For the work presented here, the body surface is considered to be continuous and smooth, with no irregularities or edges. Surface roughness and sharp edges can significantly increase the sound radiated from a TBL. These effects have not been included in the present work. Also, the intended application for the proposed $k-\varepsilon$ sound model is the prediction of flow induced noise for a slender body operating in a marine environment and hence the Mach numbers of interest are very low.

For a TBL there are several sources of sound. The fluctuating velocity in the boundary layer generates a volume distribution of quadrupole sources. The fluctuating wall pressure and surface shear stress produce surface distributions of dipole sources. Gloerfelt et al. (2005) demonstrated that the sound pressure field produced by the pressure dipole sources is equivalent to the scattering of the volume quadrupole sound field by the body. Powell (1960) showed that for a TBL over a flat, smooth surface, the pressure dipoles represent the reflection of the volume quadrupoles by the surface and the radiated sound scales in the same way as free turbulence.

The role of the surface shear stress dipole on sound production and propagation in a TBL has been the subject of debate. Landahl (1975) linked the noise radiated from a TBL to the fluctuating wall shear stresses arising from turbulent processes in the near wall region. He derived expressions relating the acoustic power radiated by both dipole and quadrupole sources to the friction velocity, u_*. He found that the acoustic power radiated by the surface shear stress dipole scaled with u_*^6 whereas the acoustic power radiated by the quadrupole scaled with u_*^8. Landahl (1975) concluded that at low Mach numbers, the surface shear stress dipole will dominate the TBL noise. In contrast, Howe (1979) presented analytical results that suggested the surface shear stress dipole was not a source of noise at all. He stated it was a propagation term that described how the wall shear flow modified the propagation of acoustic waves in the vicinity of the wall. However, Shariff and Wang (2005) conducted numerical studies demonstrating that a fluctuating surface shear stress is a valid source of sound radiation. Also, Hu et al. (2003, 2006) predicted the sound generated by direct numerical simulation of TBL flows over a smooth surface. They showed that not only are fluctuating surface shear stresses a valid source of sound radiation, they are the dominant sound source at low Mach numbers. It is important to highlight that

Hu et al. (2003, 2006) consider only smooth boundaries in their work. For a rough surface, the roughness elements act to scatter the sound produced by the volume quadrupoles. Hence the pressure dipole source term contributes significantly to the sound radiated from a rough surface. Yang and Wang (2008) studied the relative strengths of the pressure and surface shear stress dipoles for a single Reynolds number flow over a flat plate with a hemispherical roughness element. At this Reynolds number, they found that the pressure dipole term is a more dominant source of TBL noise than the shear stress dipole. However, it is unclear from the literature what the relative strengths of the pressure and shear stress dipoles are for a rough surface in the limit $M \to 0$. For the work presented here, the surfaces are considered to be smooth and flat and the Mach number is very low. Hence the TBL noise will be dominated by surface shear stress dipoles.

The proposed $k-\varepsilon$ sound model uses a volume distribution of sources based on the work of Proudman (1952) to approximate the acoustic intensity generated by turbulent fluctuations in the flow. These sources are calculated based on the k and ε fields obtained from a steady-state CFD simulation. A distribution of surface shear stress dipole sources is used to predict the acoustic intensity generated by the turbulent boundary layer. A method is derived to approximate the fluctuating wall shear stress from steady-state CFD data. From this fluctuating wall shear stress, the acoustic intensity and power generated by the surface can be estimated.

The $k-\varepsilon$ sound model is calibrated against experimental data for sound generated by a low Mach number turbulent jet, as well as numerical data of sound produced by a turbulent boundary layer. The $k-\varepsilon$ sound model is then applied to investigate the sound produced by turbulent flow past a slender body.

NUMERICAL METHODS

As a first approximation, the sources of flow noise can be represented as the sum of volume and surface components as follows:

$$\begin{aligned} P &= P_s + P_v \\ &= \int_S p_s(\mathbf{y}_b)\,dS + \int_V p_v(\mathbf{y})\,dV \end{aligned} \tag{1}$$

where P is the total acoustic power generated by the flow. $p_s(\mathbf{y}_b)$ and $p_v(\mathbf{y})$ are respectively the surface component (dipole) and volume component (quadrupole). $\mathbf{y}$ and $\mathbf{y}_b$ are the position vectors of the volumetric and surface source points, respectively. Esimates for p_s and p_v can be given as:

$$p_v(\mathbf{y}) = A\rho\varepsilon(\mathbf{y})\left(\frac{\sqrt{k(\mathbf{y})}}{c}\right)^5,\ p_s(\mathbf{y}_b) = B\rho\left(\frac{k_0(\mathbf{y}_b)}{c}\right)^3 \tag{2}$$

where c is the speed of sound and ρ is the fluid density. $k(\mathbf{y})$ and $\varepsilon(\mathbf{y})$ are the turbulent kinetic energy and dissipation rate at $\mathbf{y}$, respectively. $k_0(\mathbf{y}_b)$ is the kinetic energy of the fluctuating component of the friction velocity evaluated at $\mathbf{y}_b$. A, B are constants to be determined by model calibrations. The expression for $p_v(\mathbf{y})$ comes from the work of Proudman (1952) on the noise generated by isotropic turbulence. $p_v(\mathbf{y})$ is readily calculated using the values for k and ε from a CFD solution. The expression for $p_s(\mathbf{y}_b)$ is derived from the scaling laws of aerodynamic noise and recognising that it corresponds to a dipole noise source, as presented by Skvortsov et al. (2009).

A fluctuating wall shear stress, $\tau_w(t)$, acting on an area, A_w, produces a fluctuating force $F_\tau(t) = \tau_w(t)A_w$. Following the derivation of Goldstein (1976) (pp 124-125) for sound power generated by a fluctuating surface force, the time average acoustic intensity, $\bar{I}$ is given by:

$$\bar{I} \approx \frac{1}{16\pi c^3\rho}\frac{x_i x_j}{R^4}\overline{\frac{dF_{\tau,i}(t)}{dt}\frac{dF_{\tau,j}(t)}{dt}} \tag{3}$$

where $F_{\tau,i}(t)$ and $F_{\tau,j}(t)$ are the i^{th} and j^{th} components of the fluctuating shear force $F_\tau(t)$, respectively. x_i and x_j are, respectively, the i^{th} and j^{th} components of the position vector $\mathbf{x}$ of the field point. R is the distance between source point, $\mathbf{y}_b$ and $\mathbf{x}$. Here it is assumed that $|\mathbf{x}| >> |\mathbf{y}_b|$.

Continuing with the derivation presented by Goldstein (1976) (pp 124-125), it can be shown that:

$$\overline{\frac{dF_{\tau,i}(t)}{dt}\frac{dF_{\tau,j}(t)}{dt}} \propto \frac{1}{T_f^2}|F_\tau|^2 \tag{4}$$

where T_f is the characteristic period of the fluctuation and can be expressed as:

$$T_f \propto \frac{L}{U_c} \tag{5}$$

Here L is a characteristic length of the surface and U_c is a characteristic velocity of the flow. For a force caused by fluctuating surface shear stresses, a logical choice for the characteristic velocity is:

$$U_c = u_* \tag{6}$$

where u_* is the friction velocity. The fluctuating force due to shear stresses can be related to the friction velocity as follows:

$$\begin{aligned} |F_\tau| &\propto |\tau_w|A_w \\ &\propto \rho u_*^2 L^2 \end{aligned} \tag{7}$$

Here $A_w \propto L^2$ has been used along with the definition for friction velocity, $u_* = \sqrt{\frac{\tau_w}{\rho}}$. By recognising that both $x_i \propto R$ and $x_j \propto R$, $\bar{I}$ can be expressed as being proportional to:

$$\bar{I} \propto \frac{\rho u_*^6 L^2}{c^3 R^2} \tag{8}$$

Integrating equation (8) over a sphere of radius R gives an expression for the acoustic power:

$$\bar{P}_s \propto \frac{\rho u_*^6 L^2}{c^3} \tag{9}$$

It is only the fluctuating component of u_* in equation (9) that produces sound. A method to estimate this fluctuating component from steady-state CFD data is presented in what follows.

Define $k_0 \propto u_*^2$ as the amount of kinetic energy associated with the fluctuating component of the friction velocity. Considering a surface, S, equation (9) can be converted into the following integral equation:

$$\bar{P}_s = \int_S B\rho\left(\frac{k_0(\mathbf{y}_b)}{c}\right)^3 dS \tag{10}$$

which is the expression given in equation (2). In the standard $k-\varepsilon$ turbulence model of Launder and Spalding (1974), there is a relationship between flow shear stress, τ, and k, given by:

$$\tau = \rho\sqrt{C_\mu}k \tag{11}$$

where C_μ is a constant coefficient of the turbulence model. Using this relationship k_0 is defined as:

$$k_0(\mathbf{y}_b) = \frac{\tau_{t_0}(\mathbf{y}_b)}{\rho\sqrt{C_\mu}} \tag{12}$$

$\tau_{t_0}(\mathbf{y}_b)$ is the fluctuating component of the wall shear stress at $\mathbf{y}_b$ and is defined as:

$$\tau_{t_0}(\mathbf{y}_b) = \tau_0(\mathbf{y}_b)\frac{\nu_t}{\nu} \tag{13}$$

where $\tau_0(\mathbf{y}_b)$ is the mean wall shear stress at $\mathbf{y}_b$, ν is the viscosity of the fluid and ν_t is the turbulent, or eddy, viscosity and is taken

from the computational cell adjacent to the wall. Hence a final expression for $k_0(\mathbf{y}_b)$ is given by:

$$k_0(\mathbf{y}_b) = \frac{\tau_0(\mathbf{y}_b)\nu_t}{\rho\nu\sqrt{C_\mu}} \tag{14}$$

All quantities on the right hand side of equation (14) can readily be obtained from a steady-state CFD analysis. To approximate a value for ε on the boundary faces, ε_0, the following approach is used:

$$\varepsilon_0(\mathbf{y}_b) = \frac{C_\mu k_0^2(\mathbf{y}_b)}{\nu_t} \tag{15}$$

which is based on another relationship in the turbulence model of Launder and Spalding (1974).

Considering $p_s(\mathbf{y}_b)$ and $p_v(\mathbf{y})$ to act as point sources, the acoustic intensity, I, at a field point, $\mathbf{x}$, is determined by:

$$I(\mathbf{x}) = I_s(\mathbf{x}) + I_v(\mathbf{x}) \tag{16}$$

$I_s(\mathbf{x})$ and $I_v(\mathbf{x})$ are the acoustic intensity at a field point $\mathbf{x}$ due to the surface and volumetric sources, respectively, and are given by:

$$I_s(\mathbf{x}) = \int_S \frac{p_s(\mathbf{y}_b)}{4\pi R^2} dS(\mathbf{y}_b)\ ,\ I_v(\mathbf{x}) = \int_V \frac{p_v(\mathbf{y})}{4\pi R^2} dV(\mathbf{y}) \tag{17}$$

$R = |\mathbf{x}-\mathbf{y}|$ is the distance between the source and field points. The intensity is related to the sound pressure as follows:

$$I(\mathbf{x}) = \frac{p_a^2(\mathbf{x})}{\rho c} \tag{18}$$

where $p_a(\mathbf{x})$ is the sound pressure at $\mathbf{x}$. Hence an expression for the sound pressure is given by:

$$p_a(\mathbf{x}) = \sqrt{I(\mathbf{x})\rho c} \tag{19}$$

The spectral properties of the acoustic power, intensity and hence sound pressure can be approximated by assuming simple spectra for the volume and surface sources. For the volume sources, the spectrum is defined by:

$$f_v(\omega, q_v, r_v, C_v) = \frac{C_v\left(\frac{\omega}{\omega_0}\right)^{q_v}}{1+\left(\frac{\omega}{\omega_0}\right)^{r_v}} \tag{20}$$

where C_v is a parameter to be determined by model calibration. ω is the radian frequency. ω_0 is the characteristic frequency and here is given by:

$$\omega_0 = F_v\left(\frac{\varepsilon}{k}\right) \tag{21}$$

where F_v is a calibration prefactor. The values for q_v and r_v in equation (20) are approximated by considering the asymptotic behaviour of acoustic spectra from turbulent jets:

$$f_v(\omega, q_v, r_v, C_v) \approx \begin{cases} \left(\frac{\omega}{\omega_0}\right)^{q_v} & \frac{\omega}{\omega_0} << 1 \\ \left(\frac{\omega}{\omega_0}\right)^{q_v - r_v} & \frac{\omega}{\omega_0} >> 1 \end{cases} \tag{22}$$

For the volumetric sources, $q_v = 8$ due to the 8^{th} power scaling law for acoustic power generated by quadrupole sources derived by Lighthill (1952). At high frequencies, the acoustic spectra experience a power law decay of $-\frac{7}{2}$ and hence $q_v - r_v = -\frac{7}{2}$ and $r_v = \frac{23}{2}$.

For the surface sources, a piecewise linear spectrum is used:

$$f_s(\omega, q_s, r_s, s_s, C_s) = \begin{cases} 0.1^{(r_s-q_s)} C_s\left(\frac{\omega}{\omega_0}\right)^{q_s} & \frac{\omega}{\omega_0} < 0.1 \\ C_s\left(\frac{\omega}{\omega_0}\right)^{r_s} & 0.1 < \frac{\omega}{\omega_0} < 1 \\ C_s\left(\frac{\omega}{\omega_0}\right)^{s_s} & \frac{\omega}{\omega_0} > 1 \end{cases} \tag{23}$$

Here, ω_0 is given by:

$$\omega_0 = F_s\left(\frac{\varepsilon_0}{k_0}\right) \tag{24}$$

and the surface spectra, q_s, r_s and s_s are parameters to be determined by model calibration. The following equations are used for the acoustic power and intensity spectra:

$$P(\omega) = P_s f(\omega, q_s, r_s, s_s, C_s) + P_v f(\omega, q_v, r_v, C_v) \tag{25}$$

$$I(\mathbf{x}, \omega) = I_s f(\omega, q_s, r_s, s_s, C_s) + I_v f(\omega, q_v, r_v, C_v) \tag{26}$$

The correlation coefficients, A, B, C_v, C_s, F_v, F_s, q_s, r_s and s_s, from equations (2), (21), (24), (25) and (26) are determined through model calibration.

MODEL CALIBRATION

To obtain the parameters for the volumetric and surface acoustic sources in the proposed $k-\varepsilon$ sound model, two separate calibration studies are performed. To calibrate the volumetric source parameters, a low Mach number turbulent jet is modelled and the predicted sound is compared against experimental results of Laurendeau et al. (2008). Details of the low Mach number turbulent jet analysis is provided in the proceeding section on turbulent jet flows. To calibrate the surface source parameters, TBL flow is analysed. The predicted sound is compared with the numerical results of Hu et al. (2006). Details of the TBL calibration study is provided in the proceeding section on the turbulent boundary layer noise.

The calibration analysis for the turbulent jet was performed at a single Reynolds number and the acoustic results used for comparison are sound pressure levels (SPLs) measured at discrete points in space. Further work is required to extend the turbulent jet calibration to a range of Reynolds numbers to ensure that the derived parameters are robust. The calibration analysis for the TBL was performed at three Reynolds numbers and the sound power generated per unit area of the boundary is used for comparison.

In both calibration cases, the CFD analyses are conducted using ESI Group's CFD-ACE+ software package. The velocity-pressure form of the Navier-Stokes equations are solved by CFD-ACE+ and for these analyses, steady-state Reynolds Averaged Navier-Stokes (RANS) simulations of the flow fields are performed. The standard $k-\varepsilon$ turbulence model of Launder and Spalding (1974) is used with the improvements to the near wall turbulence production and dissipation terms given by Ciofalo and Collins (1989). The $k-\varepsilon$ turbulence model is a high Reynolds number model and relies on wall models to predict the production and dissipation of turbulence at the boundary. These high Reynolds number turbulence models require $30 < y^+ < 150$, where y^+ is the height of the CFD cell adjacent to the boundary non-dimensionalised by the friction velocity and kinematic viscosity of the fluid. For both calibration models analysed, an average of $y^+ \approx 40$ was used. The spatial distributions of k and ε are obtained from the simulations for both calibration models. For the turbulent jet calibration model, equations (19) and (26) are used to approximate the SPL spectra at the measurement points. For the TBL calibration model, equation (25) is used to approximate the sound power generated per unit area of the boundary. The parameters of the $k-\varepsilon$ sound model were then tuned to obtain a good match between the results predicted with the present method and the data from literature. Table 1 presents the values obtained for all calibration coefficients of the $k-\varepsilon$ sound model after the tuning.

Turbulent Jet Noise

A low Mach number turbulent jet was simulated at $Re_D = 300{,}000$ and $M = 0.3$ from a nozzle with a diameter of 0.05 m. For this simulation, a three-dimensional rectangular domain with dimensions $H \times W \times L = 4.6 \times 6.3 \times 9.4$ m^3 was modelled around the nozzle. These dimensions match the size of the anechoic chamber used for the experimental work of Laurendeau et al. (2008a, 2008b).

Figure 1 shows part of the CFD model in the vicinity of the nozzle exit with two cut planes showing the mesh distributions. The CFD model contained approximately 3.7 million cells and the steady state simulation ran for 17 hours on a standard computer. Calculation of the sound intensity spectra due to the volumetric sources took approximately 1.8 minutes per measurement point and a total time of 5.4 minutes. Hence the total time required to perform the steady state CFD simulation and predict the SPL for this case was approximately 17 hours.

Recently Fosso Pouangué et al. (2010) presented a high fidelity transient CFD simulation of the same low Mach number turbulent jet using LES. Acoustic source data was extracted from this LES simulation and the sound pressure field was predicted. They reported that their simulation was executed on 32 CPUs and required a total of 50,000 CPU hours, or two months, to complete. Hence the present method offers a huge reduction in computation time.

The SPL is calculated at $\theta = 30°$, $60°$ and $90°$ relative to the flow direction on a 2m arc centred at top dead centre of the nozzle exit. Figure 2 compares the SPL achieved with the current method after parameter tuning with the experimental results of Laurendeau et al. (2008). Figure 2 shows that the predicted SPL at $\theta = 30°$ matches very well with the experimental results. The overall shape of the predicted SPL at $\theta = 60°$ and $90°$ also compares reasonably well with the experimental results, however the SPL is overpredicted at these points. In particular, the difference in peak SPL between $\theta = 30°$ and $90°$ is less significant with the current $k-\varepsilon$ sound model than with the change in peak SPL at these points obtained experimentally. For high Mach number jets, Kandula and Vu (2003) show that the sound at small angles to the jet is dominated by large-scale turbulent structures, whereas at angles further from the axis, fine-scale turbulent structures dominate. A similar trend may occur in low Mach number jets but in its current form, the present $k-\varepsilon$ sound model is not able to resolve such multi-scale directivity.

Turbulent Boundary Layer Noise

Low Mach number TBL flow over a flat plate was simulated at friction Reynolds numbers of $Re_\tau = 360$, 720 and 1440. A 2D non-axisymmetric CFD model was built with dimensions $12h \times h$, where h is the boundary layer height. The bottom boundary was specified as a no-slip wall, the left and right boundaries were defined as periodic boundaries and the top boundary was assigned a 'zero stress' or 'slip' condition. The flow was driven from left to right using a body force. These dimensions, Reynolds numbers and boundary conditions match those used by Hu et al. (2006) in their numerical simulation of TBL noise from DNS flow data. The value of the body force was modified until the desired friction Reynolds number was achieved. Figure 3 shows a schematic of the CFD model that was used for the TBL simulations. The mesh density was modifed so that $y^+ \approx 40$ for all analyses.

Hu et al. (2006) present normalised power spectral density of the radiated sound pressure per unit area of wall. They also provide an equation to calculate the frequency weighted acoustic power spectrum per unit area of wall from the normalised power

Table 1: Calibration Coefficient Values

Calibration Coefficient	Volumetric	Surface
A	1.3E+04	-
B	-	6.6E-08
C	$\frac{2.27}{\omega_0}$	$\frac{1}{3.61\omega_0}$
q	8	1.2
r	$\frac{23}{2}$	-1.1
s	-	-3.5
F	2.0E+00	0.09

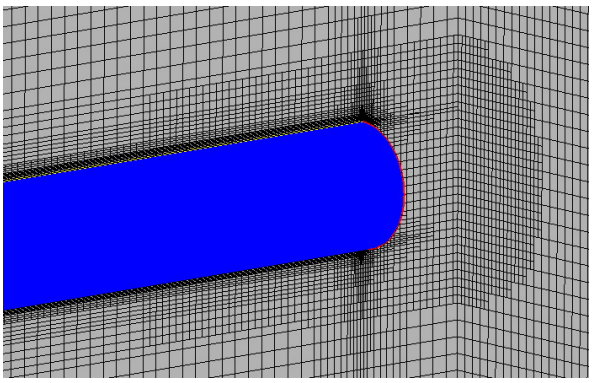

Figure 1: CFD mesh near the exit to the nozzle

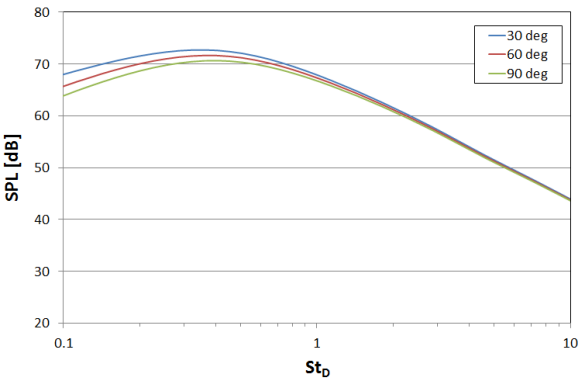

(a) SPL predicted with the present $k-\varepsilon$ sound model

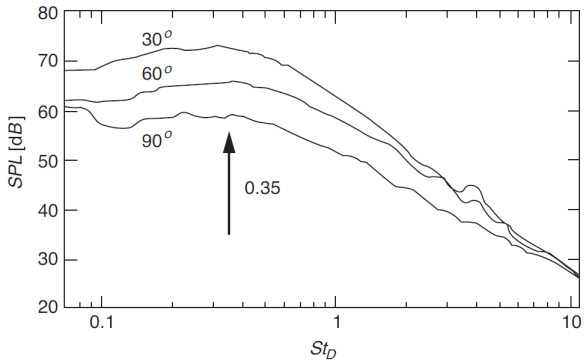

(b) SPL measured experimentally by Laurendeau et al. (2008)

Figure 2: Comparison of the turbulent jet noise between (a) the SPL predicted with the present $k-\varepsilon$ sound model and (b) experimental results by Laurendeau et al. (2008)

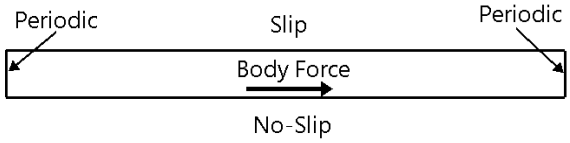

Figure 3: CFD model of the TBL over a flat plate

spectral density of pressure. Using the $k-\varepsilon$ sound model developed here, the frequency weighted acoustic power spectrum per unit area of wall was calculated. Figure 4 compares the results predicted with the current method after parameter tuning with the numerical results of Hu et al. (2006). Excellent agreement is acheived between the acoustic power spectra predicted with the current $k-\varepsilon$ sound model and the high-fidelity numerical results of Hu et al. (2006).

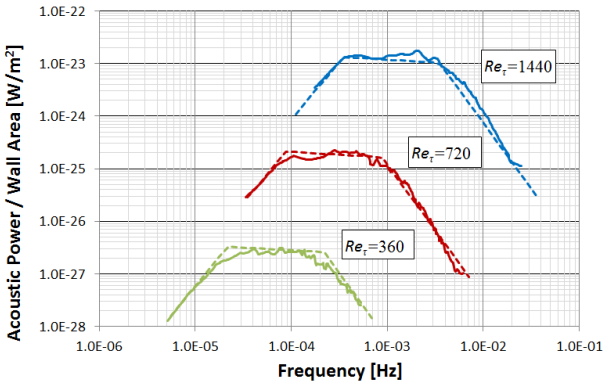

Figure 4: Acoustic power per unit wall area. Solid lines: Hu et al. (2006), Dashed lines: $k-\varepsilon$ sound model.

FLOW NOISE FROM A SLENDER BODY

High Reynolds number, low Mach number flow past an axisymmetric slender body at an angle of attack of zero degrees was then simulated. The slender body is of radius, a, and length, $L = 40a$. The flow noise generated by the slender body at Reynolds numbers ranging from 2.00E+06 to 2.05E+09 were investigated. Table 2 summarises the different simulations that were performed and the resulting computation times. Table 2 shows that the time required to perform the steady state CFD simulation and subsequent $k-\varepsilon$ sound model prediction ranges from approximately 78 minutes to 730 minutes. High fidelity simulation of the unsteady flow field using LES techniques, followed by an acoustic propagation analysis similar to that proposed by Lighthill (1952), would require significantly more computational resources. The relatively short analysis times required for the $k-\varepsilon$ sound model make it suitable for 'what-if' scenarios such as optimisation studies to reduce flow induced noise.

The distribution of k and ε were extracted from the steady state simulations. The surface and volumetric sound powers were calculated using equation (1) and the calibration parameters that were derived in the preceding section. The acoustic efficiency, η, was then calculated for each analysis. The acoustic efficiency, η, is defined as the ratio of acoustic power output to energy supplied and is given by:

$$\eta = \eta_s + \eta_v \tag{27}$$

η_s and η_v are the acoustic efficiencies of the surface and volumetric sources, respectively, and are given by:

$$\eta_s = \frac{P_s}{\rho U_\infty^3 S}\ ,\ \eta_v = \frac{P_v}{\rho U_\infty^3 S} \tag{28}$$

where U_∞ is the free stream velocity and S is the surface area of the slender body. From the work of Lighthill (1952) and Curle (1955), the acoustic efficiency of the volumetric and surfaces sources are expected to scale with the free stream Mach number as $\eta_v \propto M^5$ and $\eta_s \propto M^3$, respectively, where $M = \frac{U_\infty}{c}$. However, Landahl (1975) and Hu et al. (2006) predicted that the acoustic efficiency of sound generated by surface shear stress dipoles should scale with the friction velocity Mach number as $\eta_s \propto M_*^3$, where $M_* = \frac{u_*}{c}$. Figure 5 shows the acoustic efficiencies of the surface and volumetric sources predicted using the current $k-\varepsilon$ sound model as a function of free stream Mach number, M. Results are presented for three sound speeds, corresponding to $c = 500a$, $1000a$ and $1500a$ m/s, and show that the current method predicts a free stream Mach number scaling of $\eta_v \propto M^{4.81}$ and $\eta_s \propto M^{2.51}$, which is in reasonably close agreement to the analytical values of $\eta_v \propto M^5$ and $\eta_s \propto M^3$ predicted by Lighthill (1952) and Curle (1955). The scaling of the surface source acoustic efficiency with friction velocity Mach number was found to be $\eta_s \propto M_*^{2.75}$, which matches well with the value of $\eta_s \propto M_*^3$ predicted by Landahl (1975) and Hu et al. (2006).

Figure 6 presents the total acoustic efficiency predicted with current $k-\varepsilon$ sound model as a function of M for the three sound speeds. The dashed lines depicted in Figure 6 represent the Mach number scaling obtained from Figure 5 and the solid black line indicates when $M = C_D$. Figure 6 clearly shows that for $M << C_D$, the total acoustic efficiency becomes $\eta \approx \eta_s$. At these Mach numbers, the flow induced noise is dominated by the TBL noise. For $M >> C_D$, Figure 6 shows that $\eta \approx \eta_v$ and hence at these Mach numbers, the flow induced noise is dominated by the turbulent wake. Figure 6 also shows that for $M \approx C_D$, $\eta_S \approx \eta_V$. Hence, when evaluating flow induced noise from a slender body at $M \approx C_D$, both the surface and volumetric acoustic sources must be taken into account. By assuming $a = 1$m, the results shown in Figure 6(c) depict the relationship between η and M for a 40m vessel in a fluid with a sound speed of $c = 1500$m/s, which closely matches the speed of sound in water. For this case, the efficiency of the volumetric sources are of the same order of magnitude as the efficiency of the surface sources at $M \approx 0.003$, which corresponds to a forward velocity of 4.5 m/s. It should be stressed that the results presented here are for flat, smooth surfaces. Any roughness elements on the surface, or sharp edges such as control surface trailing edges, have not been considered. Surface roughness and sharp edges will scatter the sound generated by the volume quadrupoles and this can result in a significant increase in the far-field sound radiation. Extensions to the $k-\varepsilon$ sound model to include the effect of surface roughness and sharp edges on the radiated sound are currently being investigated.

Skvortsov et al. (2009) derived the following scaling laws for flow past a slender body:

$$P_{s_a} \approx \frac{\rho C_D^3 U_\infty^6 S}{c^3}\ ,\ P_{v_a} \approx \frac{\rho C_D^3 U_\infty^8 S}{c^5 \mu^2} \tag{29}$$

where $\mu = \frac{a}{L}$ is the slenderness ratio of the body. Both of the expressions in equation (29) scale with the cube of the drag coefficient. To compare the results obtained using the current method with these scaling laws, acoustic efficiencies for the approximate sound powers in equation (29) are obtained as follows:

$$\eta_{s_a} \approx \frac{P_{s_a}}{\rho U_\infty^3 S} = M^3 C_D^3 \tag{30}$$

$$\eta_{v_a} \approx \frac{P_{v_a}}{\rho U_\infty^3 S} = \frac{M^5 C_D^3}{\mu^2} \tag{31}$$

Introducing calibration factors into equations (30) and (31) produces the following expressions:

$$\eta_{s_a} = G M^3 C_D^3 \tag{32}$$

$$\eta_{v_a} = \frac{H M^5 C_D^3}{\mu^2} \tag{33}$$

$$\eta_a = \eta_{s_a} + \eta_{v_a} \tag{34}$$

Figure 7 shows the comparison between the acoustic efficiencies calculated from the present $k-\varepsilon$ sound model and the efficiencies based on the physics based scaling laws of Skvortsov et al. (2009) for $c = 1500a$ m/s. In Figure 7, the calibration factors are

$G = 0.002$ and $H = 0.27$. The values for G and H in Figure 7 were also found to produce similarly accurate results for $c = 500a$ and $1000a$ m/s. The acoustic efficiencies predicted using the $k-\varepsilon$ sound model agree very closely with the calibrated results from the physics based scaling laws. Hence the value predicted for η using the $k-\varepsilon$ sound model scales approximately with the cube of C_D. Such a straightforward link between the hydrodynamic drag and the flow noise generated by a slender body is an important result for shape optimisation aimed at reducing flow noise. Using this relationship, a 10% reduction in the drag acting on a body will result in a reduction of approximately 3dB in the flow noise.

CONCLUSIONS

A $k-\varepsilon$ sound model based on Proudman's formula and extended to include the sound produced by a smooth body immersed in turbulent flow has been presented. The model was calibrated against numerical and experimental data available in the literature and then applied to study the noise generated by a slender axisymmetric body subjected to high Reynolds number, low Mach number flow. The $k-\varepsilon$ sound model predicted a Mach number dependence of $\eta_s \propto M^{2.51}$ and $\eta_v \propto M^{4.81}$ for the efficiency of the surface and volumetric sound sources, respectively, which is in good agreement with the analytical values of 3 and 5. When $M << C_D$, the surface sound sources dominate the generation of sound and for $M >> C_D$, the volumetric sound sources dominate. However for $M \approx C_D$, both the surface and volumetric sources contribute appreciably to the sound generation. Also, the total acoustic efficiency predicted by the $k-\varepsilon$ sound model scales approximately with the cube of C_D.

ACKNOWLEDGEMENTS

Funding for this work has been provided by the Maritime Platforms Division of the Defence Science and Technology Organisation. Also, financial assistance from the Australian Acoustical Society (NSW Division) for an AAS NSW Travel Award to participate at the Acoustics 2011 conference is gratefully acknowledged.

REFERENCES

Ciofalo, M and Collins, MW (1989), "k-ε predictions of heat transfer in turbulent recirculating flows using an improved wall treatment", *Numerical Heat Transfer* 15, pp. 21–47.

Curle, N (1955), "The influence of solid boundaries upon aerodynamic sound", *Proceedings of the Royal Society of London A* 231, pp. 505–514.

Fosso Pouangué, A, Deniau, H, Lamarque, N, Bousuge, JF and Moreau, S (2010), "Simulation of a low-Mach, high Reynolds number jet: First step towards the simulation of jet noise control using micro-jets", *16th AIAA/CEAS Aeroacoustics Conference,* Stockholm, Sweden.

Gloerfelt, X, Pérot, F, Bailly, C and Juvé, D (2005), "Flow-induced cylinder noise formulated as a diffraction problem for low Mach numbers", *Journal of Sound and Vibration* 287, pp. 129–151.

Goldstein, ME (1976), *Aeroacoustics,* New York: McGraw-Hill.

Howe, MS (1979), "The rôle of surface shear stress fluctuations in the generation of boundary layer noise", *Journal of Sound and Vibration* 65, pp. 159–164.

Hu, Z, Morfey, CL and Sandham, ND (2003), "Sound radiation in turbulent channel flows", *Journal of Fluid Mechanics* 475, pp. 269–302.

Hu, Z, Morfey, CL and Sandham, ND (2006), "Sound radiation from a turbulent boundary layer", *Physics of Fluids* 18, p. 098101.

Kandula, M and Vu, B (2003), "On the scaling laws for jet noise in subsonic and supersonic flow", *9th AIAA/CEAS Aeroacoustics Conference, AIAA-2003-3228, Hilton Head, SC, 12-14 May.*

Landahl, MT (1975), "Wave mechanics of boundary layer turbulence and noise", *Journal of Acoustical Society of America* 57, pp. 824–831.

Launder, BE and Spalding, DB (1974), "The numerical computation of turbulent flows", *Computer Methods in Applied Mechanics and Engineering* 3, pp. 269–289.

Laurendeau, E, Jordan, P, Delville, J and Bonnet, JP (2008a), "Source-mechanism idenitification by nearfield-farfield pressure correlations in subsonic jets", *International Journal of Aeroacoustics* 7, pp. 41–68.

Laurendeau, E, Jordan, P, Bonnet, JP, Delville, J, Parnaudeau, P and Lamballais, E (2008b), "Subsonic jet noise reduction by fluidic control: The interaction region and the global effect", *Physics of Fluids* 20, p. 101519.

Lighthill, M (1952), "On sound generated aerodynamically, I. General theory", *Proceedings of the Royal Society A* 211, pp. 564–587.

Lighthill, M (1954), "On sound generated aerodynamically, II. Turbulence as a source of sound", *Proceedings of the Royal Society A* 222, pp. 1–32.

Powell, A (1960), "Aerodynamic noise and the plane boundary", *Journal of Acoustical Society of America* 32, pp. 982–990.

Proudman, I (1952), "The generation of noise by isotropic turbulence", *Proceedings of the Royal Society of London* A214, pp. 119–132.

Shannon, DW, Morris, SC and Mueller, TJ (2006), "Radiated sound and turbulent motions in a blunt trailing edge flow field", *International Journal of Heat and Fluid Flow* 27, pp. 730–736.

Shariff, K and Wang, M (2005), "A numerical experiment to determine whether surface shear-stress fluctuations are a true sound source", *Physics of Fluids* 17, p. 107105.

Skvortsov, A, Gaylor, K, Norwood, C, Anderson, B and Chen, L (2009), "Scaling laws for noise generated by the turbulent flow around a slender body", *Undersea Defence Technology: UDT Europe 2009,* pp. 182–186.

Svennberg, U and Fureby, C (2010), "Vortex-shedding induced trailing-edge acoustics", *48th AIAA Aerospace Sciences Meeting,* Orlando, Florida.

Wang, M, Moreau, S, Iaccarino, G and Roger, M (2009), "LES prediction of wall-pressure fluctuations and noise of a low-speed airfoil", *International Journal of Aeroacoustics* 8, pp. 177–198.

Yang, Q and Wang, M (2008), "Computational study of boundary-layer noise due to surface roughness", *14th AIAA/CEAS AeroAcoustics Conference,* Vancouver, Canada, AIAA Paper 2008-2905.

Table 2: Summary of the slender body CFD analyses

Re_L	U_∞ (a m/s)	CFD Cells	y^+	Time CFD [min]	Time Sound [min]
2.00E+06	5.00E-02	4.18E+05	5.72E+01	7.80E+01	5.36E-02
4.00E+06	1.00E-01	4.19E+05	5.44E+01	8.40E+01	5.37E-02
8.00E+06	2.00E-01	4.21E+05	5.05E+01	9.60E+01	5.40E-02
1.60E+07	4.00E-01	4.21E+05	4.81E+01	1.13E+02	5.41E-02
3.20E+07	8.00E-01	4.22E+05	4.58E+01	1.14E+02	5.42E-02
6.40E+07	1.60E+00	4.26E+05	4.38E+01	1.21E+02	5.46E-02
1.28E+08	3.20E+00	4.69E+05	4.21E+01	1.59E+02	6.02E-02
2.56E+08	6.40E+00	5.10E+05	4.70E+01	2.80E+02	6.54E-02
5.12E+08	1.28E+01	5.70E+05	4.90E+01	4.34E+02	7.31E-02
1.02E+09	2.56E+01	5.74E+05	4.71E+01	5.18E+02	7.36E-02
2.05E+09	5.12E+01	7.64E+05	4.89E+01	7.26E+02	9.80E-02

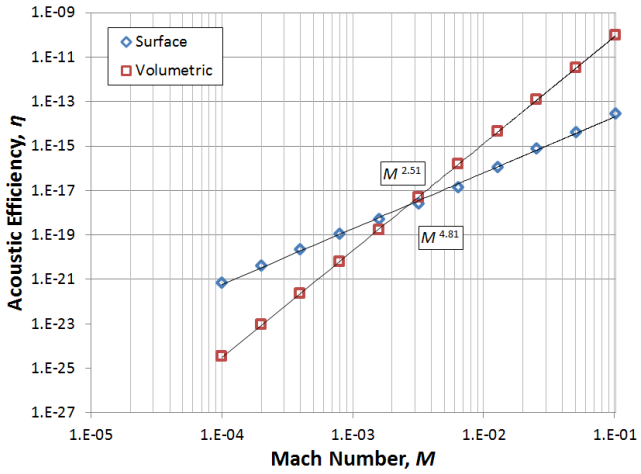

(a) $c = 500a$ m/s

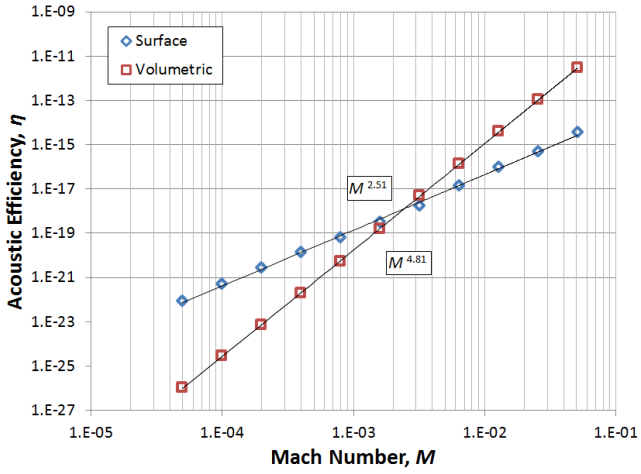

(b) $c = 1000a$ m/s

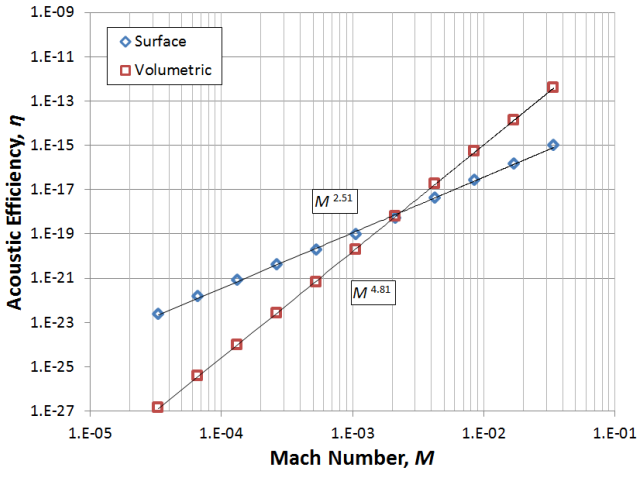

(c) $c = 1500a$ m/s

Figure 5: Acoustic efficiencies of the surface (η_S) and volumetric (η_V) sources as a function of Mach number, M

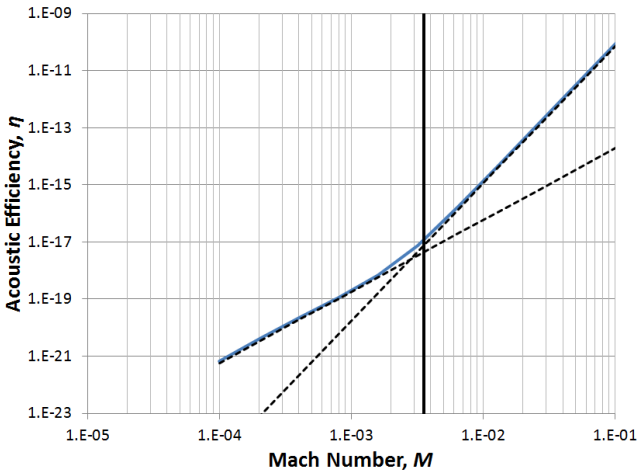

(a) $c = 500a$ m/s

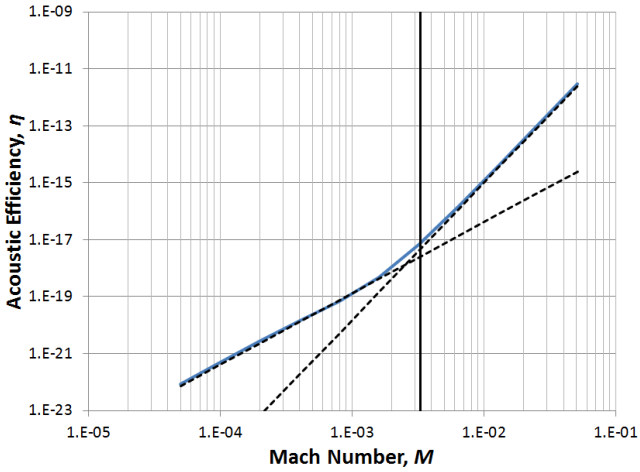

(b) $c = 1000a$ m/s

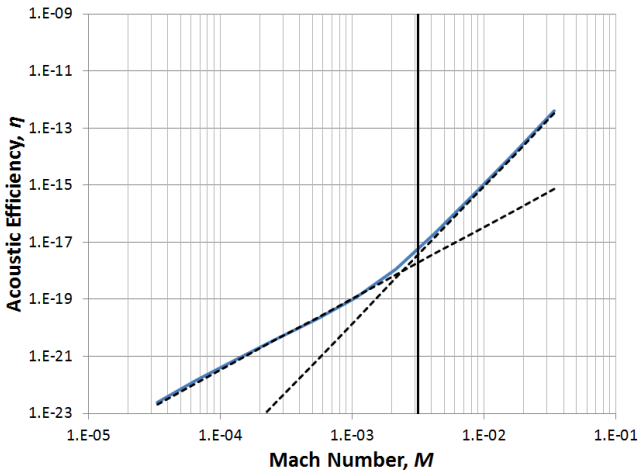

(c) $c = 1500a$ m/s

Figure 6: Acoustic efficiency as a function of Mach number, M

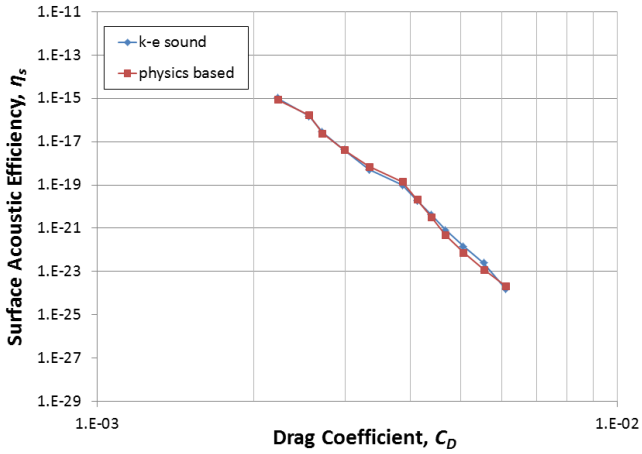

(a) Efficiency of surface sources

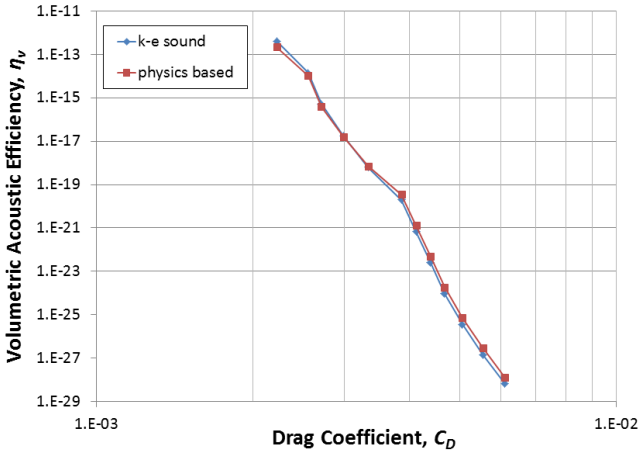

(b) Efficiency of volumetric sources

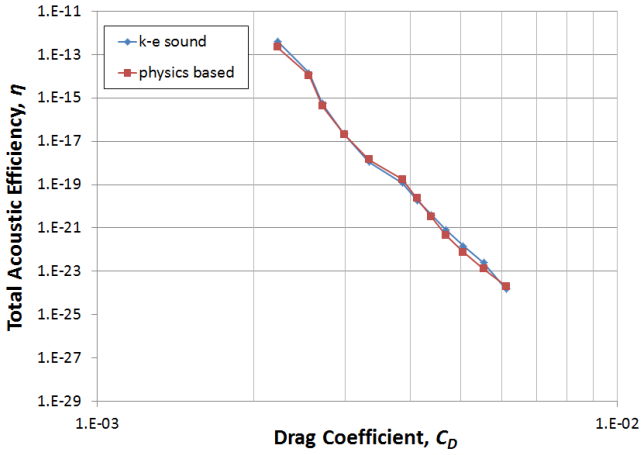

(c) Total Efficiency

Figure 7: Comparison of η and η_a for $c = 1500a$ m/s, $G = 0.08$ and $H = 0.27$